Insect wing extract: A novel source for green synthesis of nanoparticles of antioxidant and antimicrobial potential

Running Title : Green synthesis of AGNPs for use as antioxidant and antimicrobial

Parameshwar Jakinala[1#], Nageshwar Lingampally[1#], Bee Hameeda[1#], R. Z. Sayyed[2&], Yahya Khan M[3&], Elsayed Ahmed Elsayed[4,5&], Hesham El Enshasy[6,7&]

[1]Department of Microbiology, Osmania University, Hyderabad, Telangana, India

[2]Department of Microbiology, PSGVP Mandal's Arts, Science and Commerce College, Shahada, Maharashtra 425409, India

[3]Kalam Biotech Pvt. Ltd, Hyderabad, India

[4]Zoology Department, College of Science, King Saud University, Riyadh 11451, Saudi Arabia.

[5]Chemistry of Natural and Microbial Products Department, National Research Centre, Cairo1,2622, Egypt

[6]Institute of Bioproduct Development (IBD), Universiti Teknologi Malaysia (UTM), Skudai, Johor Bahru, 81310, Malaysia.

[7]City of Scientific Research and Technology Applications, New Burg Al-Arab, Alexandria, 21934, Egypt.

Corresponding author

Dr. Hameeda Bee
Assistant Professor
E-mail : drhami2009@gmail.com

[#]These authors contributed equally to this work
[&]These authors contributed equally to this work

Acknowledgments

Author Parameshwar J is thankful to UGC-RGNF [F1-17.1/2014-15/RGNF-2014-15-SC-TEL-86198] for providing research fellowship and financial support under DST-PURSE (C-DST-PURSE-II/43/2018). The authors extend their appreciation to the Deanship of Scientific Research at King Saud University for funding this work through research group No (RG-1440-053). We thank IIOR (Indian Institute of Oil Seeds Research) Rajendranagar, TS and RARS (Regional Agricultural Research Station), Anakapalle, AP for providing fungal cultures used in this study and Researcher Supporting Project, Project No. (No. RSP-2020/52), King Saud University, Riyadh, Saudi Arabia

Abstract

Silver nanoparticles (AgNPs) are among the most widely synthesized and used nanoparticles (NPs). AgNPs have been traditionally synthesized from plant extracts, cobwebs, microorganisms, etc. However, their synthesis from wing extracts of common insect; *Mang mao* which is abundantly available in most of the Asian countries has not been explored yet. We report the synthesis of AgNPs from *M. mao* wings extract and its antioxidant and antimicrobial activity. The synthesized AgNPs were spherical, 40–60 nm in size and revealed strong absorption plasmon band around at 430 nm. Highly crystalline nature of these particles as determined by Energy-dispersive X-ray analysis and X-ray diffraction further confirmed the presence of AgNPs. Hydrodynamic size and zeta potential of AgNPs were observed to be 43.9 nm and -7.12 mV, respectively. Fourier-transform infrared spectroscopy analysis revealed the presence of characteristic amide proteins and aromatic functional groups. Thin-layer chromatography (TLC) and Gas chromatography-mass spectroscopy (GC-MS) analysis revealed the presence of fatty acids in the wings extract that may be responsible for biosynthesis and stabilization of AgNPs. Further, SDS-PAGE of the insect wing extract protein showed the molecular weight of 49 kDa. *M. mao* silver nanoparticles (MMAgNPs) exhibit strong antioxidant, broad-range antibacterial and antifungal activities, which signifies their biomedical and agricultural potential.

Keywords: Antimicrobial; Antioxidant; *Mang mao*;Silver nanoparticles.

Introduction

Recent past has witnessed a significant dominance of nanotechnology in every field of human life like biomedical and engineering because it is efficient, bio-friendly, safe and economical [1]. In recent years, biologically synthesized nanoparticles are preferred over their chemical counterparts [2]. Among various nanoparticles, silver nanoparticles are widely accepted since they can be monitored easily by UV–Vis spectrophotometry [3]. Silver nanoparticles have small size, large surface area, high dispersive ability [4] and exhibit antimicrobial, anticancer, antidiabetic, antioxidant, anti-inflammatory properties [5] and are used in food processing industries, medical implants, ointment fabrication and emulsions [6]. So far, reports on green synthesis of AgNPs are from plant extracts, sea weeds, microorganisms/ metabolites and different biomaterials [7-10] are reported. However, there are no reports from wings of *Mang Mao* insects that are abundantly available and rich in proteins, polysaccharides and lipids. *M. mao* (winged termite) are eusocial insects with three groups (soldiers, workers and queen) and are commonly observed during rainy season (Figure 1a).

Figure 1 (a) *Mang Mao* insect. (b) (1) Silver nitrate solution; (2) *Mang Mao* wings extract; (3) Silver nanoparticles; (c) UV-Vis spectra of AgNPs synthesized by *Mang Mao* wings extract.

After heavy rain, these insects fly out in huge numbers during nights and get assembled near lights, and following day, shed their wings and get killed due to lack of moisture. *Mang Mao* insects are used as edible nutrient-rich and tasty food in most of the Asian countries and in rural areas they are also used to feed chickens, fish, birds and geckos. The wings of dead *M. mao* have a great environmental concern as it is a big waste. Insects' wings can be utilized as an alternative source for chitin and to synthesize nanoparticles [6, 8]. Hence, the present

study focused on biofabrication of AgNPs by using *M. mao* wings extract and evaluate antioxidant and antimicrobial potential.

Materials and Methods

Collection and preparation of *Mang mao* wings

M. mao wings used in the present study were collected during rainy season from Osmania University (17.4135º N, 78.5287º E) campus, Hyderabad, India. The wings were collected in sterilized glass beakers, aseptically washed twice with distilled water to remove dust particles, dried and stored at room temperature in air tight containers.

Synthesis of silver nanoparticles (AgNPs)

Biosynthesis of AgNPs from *Mang Mao* wings extract was carried out, following methodology given by Lateef et al.[8] *M. mao* wings (0.1 g) were hydrolyzed using 20 mL of 0.1 M NaOH at 90 ºC for 1 hour, cooled and the hydrolyzed solution was centrifuged at 8000 rpm for 10 minutes. Supernatant was collected, pH adjusted to 7 from which 1 mL of wing extract was added to 49 mL of 1 mM silver nitrate ($AgNO_3$) solution taken in 100 mL beaker and incubated at 28±1 ºC for 30 minutes under static conditions for synthesis of AgNPs. Absorption maxima was measured at 200 to 700 nm using UV-Vis spectrophotometer (HITACHI U-2900, Japan) to characterize the *Mang Mao* silver nanoparticles (MMAgNPs) and later on the sample was centrifuged at 8000 rpm for 10 min followed by pellet wash with acetone and air dried for further studies.

Optimization of MMAgNPs synthesis

Effect of various process parameters on MMAgNPs synthesis was optimized using one variable at a time (OVAT) approach [9] where, the effect of a single parameter was evaluated initially and concentration obtained was used as a standard for all the subsequent steps. Parameters optimized using OVAT included $AgNO_3$ (1 to 3 mM), the concentration ratio of

106 silver nitrate and *M. mao* wings extract (1:1, 1:3, 1:5), pH (3 to 11) and reaction time (0 to 30
107 minutes). The presence of AgNPs in the resultant solution was detected by the absorbance
108 maxima as mentioned above.

109 ### Stability study

110 Above optimized MMAgNPs were incubated at 28±1 ºC in dark conditions for 120 days and
111 absorbance maxima was measured weekly once to determine its stability

112 ## Characterization of MMAgNPs

113 Scanning electron microscopy (SEM) of the sample was performed by dispersion of the
114 sample in aluminum foil at 5.0 kV operating voltage using JSM-7500F and images were
115 recorded at different magnifications. Energy-dispersive X-ray (EDX) analysis was performed
116 by using Hitachi S-3400 NSEM instrument equipped with Thermo EDX for which the
117 synthesized MMAgNPs were dehydrated and coated on carbon film. X-ray diffraction (XRD)
118 was carried out by drop-coating MMAgNPs solution onto a glass substrate and diffraction
119 was measured using Philips X'Pert Pro X-Ray diffractometer. The average crystal size of
120 nanoparticles was estimated using Scherrer equation i.e., $D= K \lambda/\beta \cos\Theta$ [10]. The particle
121 size distribution and zeta potential of MMAgNPs was analyzed in triplicate by
122 electrophoretic light scattering at 25 °C, 150 V (DelsaMax PRO Light Scattering Analyzer,
123 Beckman Coulter, United States) in distilled water. Functional groups were determined by
124 FTIR spectroscopy (Bruker Tensor 27) and spectra were measured in the range 4000–400
125 cm^{-1} wavelength using KBr pellet as background reference.

126 Size and zeta potential of the silver nanoparticles were determined by Malvern
127 Zetasizer ZEN 3600 (United Kingdom). This instrument allows the measurement of particle
128 sized distribution in the range 2 nm–3 nm [11].

129 ### Thin layer chromatography and Gas chromatography mass spectroscopy

Reducing compounds of *M. mao* wings extract was analyzed by TLC on silica gel plates (silica gel 60 F254, Merck, Germany) with mobile phase (chloroform: methanol {97:3}), and chromatogram was examined under UV fluorescence (11). GC-MS analysis of *Mang Mao* wings extract was performed according to method as described by Ha et al.[12].

Extraction and purification of protein from *M.mao* wings

The protein from *Mang Mao* wings were extracted as per Zhang et al.[13] and precipitated using ammonium sulfate till approximately 30% saturation and incubated overnight at 4 °C followed by centrifugation. Pellet obtained was suspended in 0.05 M Tris-HCl buffer (pH – 7), with 0.1 M NaCl, and dialyzed against the same buffer for 24 h. The crude protein was filtered using a 0.22 µm membrane filter and then subjected to column chromatography using silica gel and used for synthesis of AgNPs. Crude and purified proteins were further analyzed by sodium dodecyl sulfate polyacrylamide gel electrophoresis (SDS-PAGE) and its molecular weight (Broad range 11 to 245 kDa, BioLabs, England) was determined [14].

Antioxidant and antimicrobial activity of MMAgNPs

DPPH free radical scavenging activity

Antioxidant activity of MMAgNPs was evaluated by 2, 2-diphenyl-1-picrylhydrazyl (DPPH) free radical scavenging assay [11]. Reaction mixture consisted of equal volumes (1:1 w/v) of different concentrations of the synthesized MMAgNPs (100 to 500 µg mL^{-1} in water), to which 1 mL of 0.5 mM DPPH in ethanol solution was added. The reaction mixture was incubated in dark for 30 min at 28±2 ºC. The absorbance is measured at 517 nm by UV-Vis spectrophotometer. Standard used was ascorbic acid to determine scavenging activity which was calculated by following equation.

$$\% \text{ scavenging activity} = [(A_{control} - A_{test}) / A_{control}] \times 100$$

Reducing power assay

Ferric reducing power assay was determined with 1 mL of the synthesized MMAgNPs, 2.5 mL of 0.2 M phosphate buffer (pH–6.6) and 2.5 mL of 1% potassium ferricyanide incubated at 50 ^{o}C for 20 minutes followed by cooling at room temperature. Then 2.5 mL of 10% trichloroacetic acid was added to the above mix and centrifuged at 8000 rpm for 20 min. Supernatant was mixed with distilled water in 1:1 v/v ratio and 1 mL of 0.1% ferric chloride was added and further incubated at 28± 2ºC for 10 min. Spectrophotometric absorbance of the resultant solution was measured at 700 nm. Increase in absorbance of reaction mixture indicated reducing activity of sample.

Determination of antibacterial and antifungal activity of MMAgNPS

Antibacterial activity of MMAgNPs was tested against bacteria namely *Staphylococcus aureus* MTCC 96, *Pseudomonas aeruginosa* MTCC 424, *Escherichia coli* MTCC 43, *Klebsiella pneumonia* MTCC 9751 and *Achromobacter xylosoxidans* SHB 204 (obtained from our lab) and antifungal activity was tested against *Fusarium oxysporum f. sp. ricini, Fusarium oxysporum f. sp. lycopersici* MTCC 10270*, Phytophthora nicotianae, Fusarium sacchari* and *Colletotrichum falcatum* using agar well diffusion method [15] using nutrient and potato dextrose agar plates (Fungal strains were obtained from IIOR, Hyderabad and RARS, Andhra Pradesh). Aliquots of 50 µL of different concentrations of MMAgNPs (10 µg mL^{-1}, 5 µg/mL, 2.5 µg mL^{-1} and 1.25 µg mL^{-1}) were separately added in the wells. The inoculated bacterial and fungal plates were incubated at 37 °C for 24 h and 28 °C for 72-96 h respectively and observed for inhibition of growth.

Statistical analysis

All the experiments were performed in triplicates, repeated twice and data was expressed as means ± standard deviation using Excel 2012, and graphs were drawn using Origin Pro 2015.

Results and Discussion

Synthesis of MMAgNPs

M. mao wings extract, rich in proteins, chitin and lipids was used for the reduction of $AgNO_3$ into AgNPs. The change in color of reaction mixture from yellow to dark brown after 30 minutes incubation (Figure 1) indicated synthesis of MMAgNPs. The intensity of dark brown colour change indicated AgNPs formation from silver salt which is due to excitation of surface plasmon resonance (SPR) effect [16].

Optimization of MMAgNPs synthesis

During the optimization study using OVAT, $AgNO_3$ when used at 1 mM concentration showed maximum absorption at 430 nm, indicated active formation of MMAgNPs. Further increase in the concentration of $AgNO_3$ resulted in decreased absorption (Figure 2a). These results were in agreement with the previous investigations carried out as per Veerasamy et al. [17]. When, *M. mao* wings extract (1 mL) was added to $AgNO_3$ solution (1 mM), rapid conversion to brown color observed within 30 minutes, indicated active MMAgNPs synthesis (Figure 2b). The increased color change of brown color was directly proportional to the incubation period which is due to reduction of $AgNO_3$ and excitation of SPR [16]. The absorption peak varied with different pH and it ranged between 390-470 nm (Figure 2c). The MMAgNPs formation was found to be slow at acidic pH (2-5). At neutral pH (7) absorption maxima was observed at 430 nm and the reaction started as soon as $AgNO_3$ was added to the reaction mixture. The change in color to brown was observed within 30 minutes which indicated MMAgNPs synthesis (Figure 2d).

Figure 2 (a) UV–vis spectra of aqueous silver nitrate concentration. (b) Concentration ratio of *Mang Mao* extract with 1 mM silver nitrate. (c) Different pH range. (d) Different time intervals

Further, beyond pH 7 MMAgNPs resulted in aggregation and fall in flocculation. Previous studies revealed that at alkaline pH, Ag (I) ions in solution partly hydrolyze to form bioorganic-Ag(OH)x or bioorganic-$Ag(NH_3)_2$ complex on the surface of the particle and $AgOH/Ag_2O$ colloid in the medium [18]. The characteristic absorption peak at 430 nm corresponded to SPR of AgNPs previously reported by Bahrami-Teimoori et al. [19], which thereby confirmed the synthesis of MMAgNPs. This indicates the significance of *M. mao* wings extract in the reduction of metal salts to their respective metal nano-particles.

Stability study of MMAgNPs

The stability of MMAgNPs was monitored up to 120 days (weekly once) and there was no change in absorbance at 430 nm (data not shown). This indicated strong stability of biosynthesized MMAgNPs which might be attributed to presence of carboxylate group in proteins that may result in stable nanoparticles [20].

Characterization of MMAgNPs

UV–visible spectroscopic analysis of MMAgNPs

Nanoparticles synthesis is generally found to occur due to excitation of surface plasmon resonance (SPR) [21]. The strongest absorption peak observed at 430 nm (Figure 1c) corresponds to SPR of AgNPs which is in accordance with previous reports [22, 23].

SEM and EDX analysis of MMAgNPs

SEM analysis revealed the occurrence of MMAgNPs in a spherical shape and their size ranged between 40 to 60 nm. The results showed that variation of pH in reaction mixture altered the nanoparticles size (Figure 3), however, at neutral pH the nanoparticles were uniform (Figure 3). Reddy et al. [24] reported that biosurfactants (surfactin) used for AgNPs synthesis altered the pH and decreased AgNPs size (9.7 to 4.9 nm) and at pH-9 the nano-particles were uniform. However, MMAgNPs were not uniform in size, and variations in nanoparticle's size were reported by Ahmed et al. [25] and Narayan and Dipak [26] using

plant and seaweed extracts. The EDX spectra of MMAgNPs revealed the presence of characteristic signals of silver ions at 3keV (Figure 4a) similar to those observed with chemically synthesized AgNPs. The emission energy at 3 keV indicated the reduction of silver ions to elemental silver [27].

Figure 3 SEM images (a) pH-3. (b) pH-5. (c) pH-7. (d) pH-9. (e) pH-11

XRD analysis of MMAgNPs

The XRD pattern of MMAgNPs showed the diffraction peaks at 2θ values of 32.6°, 46.57°, 67.8° and 77.04° which further confirmed crystalline nature of MMAgNPs (Figure 4b) and corresponded to standard JCPDS file No. 04-0783 [28]. Broadening in peaks occurred due to smaller particle size, which reflects the experimental conditions on nucleation and growth of crystal nuclei [29]. According to Debye Scherrer equation, the average nanoparticle size in this study was found to be 32 nm, which was relatively similar as described earlier by Sri Ramkumar et al.[30].

Figure 4 (a) Energy dispersive X-ray analysis of the synthesized MMAgNPs. (b) XRD pattern of biosynthesized silver nanoparticles using *Mang Mao* wings extract.

Zeta potential

Particle size distribution and zeta potential of MMAgNPs was depicted in Figure 5a & 5b. Average particle size of synthesized MMAgNPs was 43.9 nm and zeta potential -7.12 mV. The negative charges on AgNPs might be due to *Mang Mao* wings extract covering on nanoparticles. For the determination of overall surface charges on nanoparticles zeta potential analysis was applied.

Figure 5 Characterization of MMAgNPs by (a) DLS size distribution and (b) zeta potential analysis

Stability and prevention of aggregate formation, attributed to repulsions, due to same charge is provided by positive or negative charge on surface of nanoparticles [31]. This indicates better stability of nanoparticles and prevents agglomeration [32]. Hydrodynamic size and zeta potential of MMAgNPs in this study, corroborate with recent report of Badoei-dalfard et al. [33] hydrodynamic size (30-50 nm) of AgNPs synthesized using uricase from *Alcaligenes faecalis* GH3 and zeta potential (-4.6 mV) using *Madhuca longifolia* flower extract [31].

FTIR analysis

Identification of bond linkages and functional groups involved in reduction and stability AgNPs synthesis were performed using FTIR. The FTIR spectra of *M. mao* wings extract and synthesis of AgNPs is shown in Figure 6. *M. mao* wings extract bands observed at 3383, 1740, 1641, 1369, 1211, 1049 and 892 cm^{-1}, which is related to stretching vibrations of OH of carboxylic acids, C=O of ester fatty acid group, C=O of amide band, C-H of aliphatic bending group, C-O-C of polysaccharide, C-O stretching and –C=O of inorganic carbonate respectively.

Figure 6 FTIR pattern of the *Mang Mao* wings extract and synthesized MMAgNPs

After reduction, AgNPs form the bands observed at 3291, 2885-2828, 1801, 1643, 1552, 1403, 1322, 1046 and 650 cm^{-1} which is related to stretched vibrations of OH of carboxylic acids, C-H of aliphatics, C=O of anhydride, C=O of amide bond, C=C aromatic, CH of aliphatic bending group, NO_2 stretch, C-O stretching and N-H stretch respectively. Biomolecules present in the *M. mao* wings extract might be responsible for synthesis and

stability of AgNPs. The characteristic FTIR peaks observed in the present study were similar to those reported by Dhanasekaran et al.[34] and Usha et al. [35]. Similar results were reported by Selvakumar et al.[36] and Soman and Ray [37] where synthesis is performed using *Acalypha hispida* and *Ziziphus oenoplia* (L.) leaf extract as reducing and stabilizing agent.

TLC of Mang Mao wings extract

TLC analysis of *Mang Mao* wings extract corresponded to Rf value 0.96 which is similar to insect chemicals based on previous studies [38]. These chemicals may also be responsible for biofabrication of MMAgNPs (Figure 7a).

Figure 7 (a) TLC of *Mang Mao* wings extract: (1) UV visualization, (2) Ninhydrin reagent. (b) SDS-PAGE analysis of *Mang Mao* wings extract protein; Lane 1. Molecular size marker; lane 2. Crude protein; lane 3. Purified protein (46 kDa) responsible for active biosynthesized MMAgNPs

Gas chromatography mass spectrometric analysis

GC–MS data revealed that *M.mao* wings extract have 30 major compounds with their molecular weight shown in Table 1. Major components of wings are comprised by aliphatic hydrocarbons and are 9-Octadecynoic acid (16.9%), Nonadecanoic acid (11.4), Ethyl 9-octadecenoate (9.8%), Heptacosanoic acid (4.9%), 1-[2-Deoxy-.beta.-d-erythro-pentofuranosyl] p (4.6%), Hexadecanoic acid (3.7%), 3-Nonyn-2-ol (3.7%), 8-acetoxy-6-benzenesulfonyl-2-th (3.2%), Ethanone (3.1%), 1,5-Cyclooctadiene (3%). These components may be responsible for the reduction and capping of silver ions. Octadecynoic acid and hexadecanoic acid are fatty acids that are widely observed in insects, plants and animals [39-41]. These fatty acids are situated within wings membrane under the epicuticular surface [12,

41]. The components present in *Mang Mao* wings extract corresponds with that of previous reports on nanoparticles synthesis [36, 42, 43].

Table 1. GC-MS analysis of *M. mao* wings extract

Peak	Retention Time	Peak Area	Area (%)	Peak Height	Base m/z	Compounds present
1	4.293	16038	2.80	5062	43.95	Aspidospermidine-3-carboxylic acid, 2,3-dide
2	7.462	9307	1.63	4568	43.90	Histidine, 4-nitro-
3	10.765	8152	1.42	4045	333.80	trans-5-Hydroxytricyclo[4.4.0.0(3,8)]-4-carbo
4	11.670	6678	1.17	1309	42.90	5-Pyrimidinecarboxylic acid, hexahydro-5-(1-
5	13.051	18391	3.21	4402	43.95	Acetic acid, 8-acetoxy-6-benzenesulfonyl-2-th
6	15.405	6944	1.21	3476	43.90	p-Chlorocinnamide
7	16.978	13566	2.37	4121	58.90	2,5,7-Metheno-3H-cyclopenta[a]pentalen-3-o
8	17.055	17249	3.01	1863	40.00	1,5-Cyclooctadiene
9	17.287	18141	3.17	5052	43.90	Ethanone, 1-(4-pyridinyl)-, oxime
10	17.320	26832	4.69	5182	43.90	1-[2-Deoxy-.beta.-d-erythro-pentofuranosyl]p
11	17.554	65501	11.44	26163	88.00	Nonadecanoic acid, ethyl ester
12	19.309	96933	16.94	43045	66.95	9-Octadecynoic acid
13	19.366	56171	9.81	24672	54.95	Ethyl 9-octadecenoate, (E)-
14	19.405	7072	1.24	6466	43.95	3-p-Toluenesulfonyl-7-hydroxymethyl-9-hydr
15	19.634	21515	3.76	12272	330.11	Hexadecanoic acid
16	21.610	12089	2.11	3085	43.95	Scilliroside
17	21.909	8632	1.51	3507	66.90	Cyclohexanol, 2-butyl-
18	22.146	10102	1.77	3802	43.95	6-Benzenesulfonyl-2-oxa-6-aza-adamantane-
19	22.980	9703	1.70	6415	73.10	Heptasiloxane, hexadecamethyl-
20	23.045	10758	1.88	3399	44.00	N-[2,2,2-Trifluoro-1-(isopropylamino)-1-(trifl
21	23.390	10906	1.91	1134	43.90	Carboethoxy-1-piperazinethiocarboxylic acid
22	23.520	6339	1.11	2346	43.85	Acetamide, 2,2-dichloro-
23	24.200	21662	3.78	3185	43.05	3-Nonyn-2-ol
24	24.830	9090	1.59	4327	53.00	2-Chloro-3-(chloromethyl)-4-pentenoic acid,
25	24.923	13120	2.29	4364	41.00	Butanoic acid, 3-bromo-, ethyl ester
26	26.067	14088	2.46	3903	42.95	3-Cyclopentene-1-propanoic acid, 5-(methox
27	26.337	28275	4.94	6648	43.05	Heptacosanoic acid, methyl ester
28	26.526	7775	1.36	3530	40.10	1(2H)-Naphthalenone, 4-ethoxyoctahydro-, tr
29	27.795	13904	2.43	3102	95.90	2-Monooleoylglycerol trimethylsilyl ether
30	30.559	7400	1.29	4819	73.00	3-Isopropoxy-1,1,1,5,5,5-hexamethyl-3-(trime

Extraction and purification of Mang Mao wings extract

SDS-PAGE analysis revealed the presence of different cellular proteins with molecular weights that ranged between 22-245 kDa. Protein band corresponded to 46 kDa (Figure 7b) was found to act as a capping agent for stabilization of the MMAgNPs.

Khan and Ahmad [44] reported, purified sulfite reductase enzyme with molecular weight of 43 kDa to be responsible for gold nanoparticles stability and synthesis. Kumar et al. [45] also claimed protein of 35.6 kDa is responsible for biosynthesis and capping agent of gold nanoparticles. However, further studies are required towards characterization and identification of this protein to validate this result.

Antioxidant activity of MMAgNPs

MMAgNPs exhibited DPPH scavenging activity in the range of 66.8 to 87.0% and in case of ascorbic acid it was found to be in the range of 89.7 to 95.5% (Figure 8a). Difference in the activity can be attributed to a different functional group attached to them. MMAgNPs showed good ferric ion reducing activity which was comparable to that of standard ascorbic acid (Figure 8b). Results obtained from this study suggested the use of biosynthesized MMAgNPs as natural antioxidants. Free radical scavenging activity of MMAgNPs is mainly due to the donation of hydrogen molecules, such as proteins, polyphenols and other biomolecules present in the colloidal solution of AgNPs [23]. Radical scavenging activity of AgNPs is due to presence of bioreductant molecules on surface of nanoparticles increasing the surface area for antioxidant activity [11]. Therefore, these MMAgNPs can be employed as a natural antioxidant in the pro-oxidants, antioxidants and to balance reactive oxygen species (ROS) levels. Previous study of AgNPs synthesized using *Catharanthus roseus* showed radical scavenging activity and prevented human cell damage and degenerative diseases [46]. This work concludes the use of MMAgNPs as potential agent of antioxidant formulations in biomedical/ pharmaceutical areas.

Figure 8 Antioxidant activity: (a) DPPH scavenging activity. (b) Ferric reducing antioxidant activity.

Antimicrobial activity of MMAgNPs

Biosynthesized MMAgNPs exhibited potential antibacterial and antifungal activity. MMAgNPs showed maximum zone of inhibition of 35±0.4 mm and minimum zone of inhibition of 16±0.2 mm against *Staphylococcus aureus* MTCC 96 and *Achromobacter xylosoxidans* SHB 204 respectively, when used at a concentration of 10 μgmL^{-1} and the results of the same are shown in Figure 9. Whereas, maximum percentage of inhibition of 86.6±0.4 mm and minimum percentage of inhibition of 62.7±0.4 mm was recorded against *Fusarium oxysporum f. sp. ricini* and *Colletotrichum falcatum* respectively when the MMAgNPs were used at a concentration of 10 $\mu g\ mL^{-1}$. MMAgNPs served as potential antibacterial, antifungal agents and may emerge as an alternative to conventional antibiotics [47].

Figure 9. Antimicrobial activity of synthesized MMAgNPs

These AgNPs due to their small size can adhere to bacterial cell membrane, increase permeability and can cause structural changes in bacteria. In case of fungi, AgNPs disrupt the membrane integrity and fungal spores leading to cell death [48]. Some researchers claimed that AgNPs enter the microorganisms and can cause damage by interacting with DNA and proteins, resulting in apoptosis [49].

Conclusion

In this study, we explored *M. mao* wings extract as an eco-friendly, cost-effective and novel biomaterial for biofabrication of AgNPs. This is the first report on use of *M. mao* (seasonal insect) wings with metal chelating potential can be used as natural reducing agents for the synthesis of nanoparticles. Antioxidant and antimicrobial properties of MMAgNPs may further widen their application in the biomedical and agricultural sectors.

Contributors

Conceptualization; HB.; Methodology, PJ and NL; Validation, HB and HE; formal analysis, PJ and NL; Investigation, PJ and NL, YA; writing—original draft preparation, HB and RA.; writing—RZS, AS and HE; supervision, HB.; project administration, HB; funding acquisition, AA, MA and HE.

References

[1]. Abdelghany, T M, Aisha M. H. Al-Rajhi, Mohamed A. Al Abboud, M. M. Alawlaqi, A. Ganash Magdah, Eman A. M. Helmy, Ahmed S. Mabrouk. Recent advances in green synthesis of silver nanoparticles and their applications: about future directions. A Review. Bionanoscience. BioNanoScience; 2018; 8: 5–16. doi:10.1007/s12668-017-0413-3

[2]. Agnihotri S, Mukherji S, Mukherji S. Immobilized silver nanoparticles enhance contact killing and show highest efficacy: Elucidation of the mechanism of bactericidal action of silver. Nanoscale. 2013;5: 7328–7340. doi:10.1039/c3nr00024a

[3]. Ahmed S, Saifullah, Ahmad M, Swami BL, Ikram S. Green synthesis of silver nanoparticles using *Azadirachta indica* aqueous leaf extract. J Radiat Res Appl Sci. Elsevier Ltd; 2016;9: 1–7. doi:10.1016/j.jrras.2015.06.006

[4]. Al-Shmgani HSA, Mohammed WH, Sulaiman, Saadoon AH. Biosynthesis of silver nanoparticles from *Catharanthus roseus* leaf extract and assessing their antioxidant, antimicrobial, and wound-healing activities. Artif Cells, Nanomedicine Biotechnol. 2017;45: 1234–1240. doi:10.1080/21691401.2016.1220950

[5]. Badoei-dalfard A, Shaban M, Karami Z. Characterization, antimicrobial, and antioxidant activities of silver nanoparticles synthesized by uricase from *Alcaligenes faecalis* GH3. Biocatal Agric Biotechnol. Elsevier Ltd; 2019; 101257. doi:10.1016/j.bcab.2019.101257

[6]. Bahrami-Teimoori B, Nikparast Y, Hojatianfar M, Akhlaghi M, Ghorbani R, Pourianfar HR. Characterisation and antifungal activity of silver nanoparticles biologically synthesised by *Amaranthus retroflexus* leaf extract. J Exp Nanosci. Taylor & Francis; 2017;12: 129–139. doi:10.1080/17458080.2017.1279355

[7]. Baker C, Pradhan A, Pakstis L, Pochan D, Shah SI. Synthesis and antibacterial properties of silver nanoparticles. J Nanosci Nanotechnol. 2005;5: 244–249. doi:10.1166/jnn.2005.034

[8]. Basu S, Maji P, Ganguly J. Rapid green synthesis of silver nanoparticles by aqueous extract of seeds of Nyctanthes arbor-tristis. Appl Nanosci. Springer Berlin Heidelberg; 2016; 1–5. doi:10.1007/s13204-015-0407-9

[9]. Belle Ebanda Kedi P, Eya'ane Meva F, Kotsedi L, Nguemfo EL, Bogning Zangueu C, Ntoumba AA, Hamza Elsayed A M, Alain Bertrand D, Malik M. Eco-friendly synthesis, characterization, in vitro and in vivo anti-inflammatory activity of silver nanoparticle-mediated *Selaginella myosurus* aqueous extract. Int J Nanomedicine. 2018;Volume 13: 8537–8548. doi:10.2147/IJN.S174530

[10]. Buckner JS, Hagen MM. Triacylglycerol and phospholipid fatty acids of the silverleaf whitefly : composition and biosynthesis. Arch Insect Biochem Physiol. 2003;79: 66–79. doi:10.1002/arch.10086

[11]. Chandrasekhar N, Vinay SP. Yellow colored blooms of *Argemone mexicana* and *Turnera ulmifolia* mediated synthesis of silver nanoparticles and study of their antibacterial and antioxidant activity. Appl Nanosci. Springer Berlin Heidelberg; 2017;7: 851–861. doi:10.1007/s13204-017-0624-5

[12]. Chowdhury S, Basu A, Kundu S. Green synthesis of protein capped silver nanoparticles from phytopathogenic fungus *Macrophomina phaseolina* (Tassi) Goid with antimicrobial properties against multidrug-resistant bacteria. Nanoscale Res Lett. 2014;9: 1–11. doi:10.1186/1556-276X-9-365

[13]. Dey A, Purkait MK. Effect of fatty acid chain length and concentration on the structural properties of the coated CoFe 2 O 4 nanoparticles. J Ind Eng Chem. The Korean

Society of Industrial and Engineering Chemistry; 2014; doi:10.1016/j.jiec.2014.09.027

[14]. Dhanasekaran D, Latha S, Saha S, Thajuddin N, Panneerselvam A. Extracellular biosynthesis, characterisation and in-vitro antibacterial potential of silver nanoparticles using Agaricus bisporus. J Exp Nanosci. 2013;8: 579–588. doi:10.1080/17458080.2011.577099

[15]. Franci G, Falanga A, Galdiero S, Palomba L, Rai M, Morelli G, Galdiero M. Silver nanoparticles as potential antibacterial agents. Molecules. 2015;20: 8856–8874. doi:10.3390/molecules20058856

[16]. Ghaffari-Moghaddam M, Hadi-Dabanlou R. Plant mediated green synthesis and antibacterial activity of silver nanoparticles using Crataegus douglasii fruit extract. J Ind Eng Chem. The Korean Society of Industrial and Engineering Chemistry; 2014;20: 739–744. doi:10.1016/j.jiec.2013.09.005

[17]. Gołębiowski M, Boguś MI, Paszkiewicz M, Stepnowski P. Cuticular lipids of insects as potential biofungicides: Methods of lipid composition analysis. Anal Bioanal Chem. 2011;399: 3177–3191. doi:10.1007/s00216-010-4439-4

[18]. Govindappa M, Hemashekhar B, Arthikala MK, Ravishankar Rai V, Ramachandra YL. Characterization, antibacterial, antioxidant, antidiabetic, anti-inflammatory and antityrosinase activity of green synthesized silver nanoparticles using *Calophyllum tomentosum* leaves extract. Results Phys. 2018;9: 400–408. doi:10.1016/j.rinp.2018.02.049

[19]. Ha S, Nguyen T, Webb HK, Hasan J, Tobin MJ, Crawford RJ, Ivanova EP. Dual role of outer epicuticular lipids in determining the wettability of dragonfly wings. Colloids Surfaces B Biointerfaces. Elsevier B.V.; 2013;106: 126–134. doi:10.1016/j.colsurfb.2013.01.042

[20]. Iijima M, Kawaharada Y, Tatami J. Effect of fatty acids complexed with polyethyleneimine on the flow curves of TiO 2 nanoparticle / toluene suspensions. Integr Med Res. Taibah University; 2016;4: 277–281. doi:10.1016/j.jascer.2016.05.003

[21]. Kagithoju S, Godishala V, Nanna RS. Eco-friendly and green synthesis of silver nanoparticles using leaf extract of *Strychnos potatorum* Linn.F. and their bactericidal activities. 3 Biotech. Springer Berlin Heidelberg; 2015;5: 709–714. doi:10.1007/s13205-014-0272-3

[22]. Khan SA, Ahmad A. Enzyme mediated synthesis of water-dispersible, naturally protein capped, monodispersed gold nanoparticles; Their characterization and mechanistic aspects. RSC Adv. 2014;4: 7729–7734. doi:10.1039/c3ra43888k

[23]. Krishnaraj C, Jagan EG, Rajasekar S, Selvakumar P, Kalaichelvan PT, Mohan N. Synthesis of silver nanoparticles using *Acalypha indica* leaf extracts and its antibacterial activity against water borne pathogens. Colloids Surfaces B Biointerfaces. 2010;76: 50–56. doi:10.1016/j.colsurfb.2009.10.008

[24]. Kumar SA, Abyaneh MK, Gosavi SW, Kulkarni SK, Ahmad A, Khan MI. Sulfite reductase-mediated synthesis of gold nanoparticles capped with phytochelatin. Biotechnol Appl Biochem. 2007;47: 191–5. doi:10.1042/BA20060205

[25]. Kumar V, Gundampati RK, Singh DK, Jagannadham M V., Sundar S, Hasan SH. Photo-induced rapid biosynthesis of silver nanoparticle using aqueous extract of *Xanthium strumarium* and its antibacterial and antileishmanial activity. J Ind Eng Chem. The Korean Society of Industrial and Engineering Chemistry; 2016;37: 224–236. doi:10.1016/j.jiec.2016.03.032

[26]. Kuyumcu E. Natural product research : formerly natural product letters chemical composition and antimicrobial activity of essential oil of *Achillea cretica* L . (Asteraceae) from. Nat Prod Res. 2012;26: 37–41.

[27]. Lateef A, Ojo SA, Azeez MA, Asafa TB, Yekeen TA, Akinboro A, I. C. Oladipo, E. B. Gueguim-Kana, L. S. Beukes. Cobweb as novel biomaterial for the green and eco-friendly synthesis of silver nanoparticles. Appl Nanosci. Springer Berlin Heidelberg; 2016;6: 863–874. doi:10.1007/s13204-015-0492-9

[28]. Mohanta YK, Nayak D, Biswas K, Singdevsachan SK, Abd Allah EF, Hashem A, Alqarawi AA, Yadav D, Mohanta TK. Silver nanoparticles synthesized using wild mushroom show potential antimicrobial activities against food borne pathogens. Molecules. 2018;23: 1–18. doi:10.3390/molecules23030655

[29]. Narayan S, Dipak S. Green synthesis of silver nanoparticles using fresh water green alga *Pithophora oedogonia* (Mont .) Wittrock and evaluation of their antibacterial activity. Appl Nanosci. 2015; 703–709. doi:10.1007/s13204-014-0366-6

[30]. Netala VR, Kotakadi VS, Bobbu P, Gaddam SA, Tartte V. Endophytic fungal isolate mediated biosynthesis of silver nanoparticles and their free radical scavenging activity and anti microbial studies. 3 Biotech. Springer Berlin Heidelberg; 2016;6: 1–9. doi:10.1007/s13205-016-0433-7

[31]. Oves M, Khan MS, Zaidi A, Ahmed AS, Ahmed F, Ahmad E, Sherwani A, Owais M, Azam A. Antibacterial and cytotoxic efficacy of extracellular silver nanoparticles biofabricated from chromium reducing novel OS4 strain of *Stenotrophomonas maltophilia*. PLoS One. 2013;8. doi:10.1371/journal.pone.0059140

[32]. Patil MP, Singh RD, Koli PB, Patil KT, Jagdale BS, Tipare AR, Kim GD. Antibacterial potential of silver nanoparticles synthesized using *Madhuca longifolia* flower extract as a green resource. Microb Pathog. Elsevier Ltd; 2018; doi:10.1016/j.micpath.2018.05.040

[33]. Rafique M, Sadaf I, Rafique MS, Tahir MB. A review on green synthesis of silver nanoparticles and their applications. Artif Cells, Nanomedicine Biotechnol. Informa UK Limited, trading as Taylor & Francis Group; 2017;45: 1272–1291. doi:10.1080/21691401.2016.1241792

[34]. Rane AN, Baikar V V., Ravi Kumar D V., Deopurkar RL. Agro-industrial wastes for production of biosurfactant by *Bacillus subtilis* ANR 88 and its application in synthesis of silver and gold nanoparticles. Front Microbiol. 2017;8: 1–12. doi:10.3389/fmicb.2017.00492

[35]. Reddy AS, Chen CY, Baker SC, Chen CC, Jean JS, Fan CW, Chen RH Chen JW. Synthesis of silver nanoparticles using surfactin: A biosurfactant as stabilizing agent. Mater Lett. Elsevier B.V.; 2009;63: 1227–1230. doi:10.1016/j.matlet.2009.02.028

[36]. Selvakumar P, Sithara R, Viveka K, Sivashanmugam P. Green synthesis of silver nanoparticles using leaf extract of *Acalypha hispida* and its application in blood compatibility. J Photochem Photobiol B Biol. Elsevier B.V; 2018;182: 52–61. doi:10.1016/j.jphotobiol.2018.03.018

[37]. Shahverdi AR, Fakhimi A, Shahverdi HR, Minaian S. Synthesis and effect of silver nanoparticles on the antibacterial activity of different antibiotics against *Staphylococcus aureus* and *Escherichia coli.* Nanomedicine Nanotechnology, Biol Med. 2007;3: 168–171. doi:10.1016/j.nano.2007.02.001

[38]. Siddiqi KS, Husen A, Rao RAK. A review on biosynthesis of silver nanoparticles and their biocidal properties. J Nanobiotechnology. BioMed Central; 2018;16. doi:10.1186/s12951-018-0334-5

[39]. Simpson RJ. SDS-PAGE of Proteins. Cold Spring Harb Protoc.2006: pdb.prot4313. doi:10.1101/pdb.prot4313

[40]. Singh P, Kim YJ, Singh H, Wang C, Hwang KH, Farh ME, Chun DY. Biosynthesis, characterization, and antimicrobial applications of silver nanoparticles. Int J Nanomedicine. 2015;10: 2567–2577. doi:10.2147/IJN.S72313

[41]. Soman S, Ray JG. Silver nanoparticles synthesized using aqueous leaf extract of *Ziziphus oenoplia* (L.) Mill: Characterization and assessment of antibacterial activity. J Photochem Photobiol B Biol. Elsevier B.V.; 2016;163: 391–402. doi:10.1016/j.jphotobiol.2016.08.033

[42]. Sri Ramkumar SR, Sivakumar N, Selvakumar G, Selvankumar T, Sudhakar C, Ashok kumar B, Karthi S. Green synthesized silver nanoparticles from: Garcinia imberti bourd and their impact on root canal pathogens and HepG2 cell lines. RSC Adv. Royal Society of Chemistry; 2017;7: 34548–34555. doi:10.1039/c6ra28328d

[43]. Tóth IY. Silver nanoparticles : aggregation behavior in biorelevant conditions and its impact on biological activity. Int J Nanomedicine. 2019;14: 667–687.

[44]. Usha Rani S, Jeeva Pandian K, Reddy BSR. Syntheses and characterisation of silver nanoparticles in the acrylate copolymers. J Exp Nanosci. 2009;4: 285–299. doi:10.1080/17458080903115338

[45]. Varadavenkatesan T, Selvaraj R, Vinayagam R. Green synthesis of silver nanoparticles using *Thunbergia grandiflora* flower extract and its catalytic action in reduction of Congo red dye. Mater Today Proc. Elsevier Ltd; 2019; 10–13. doi:10.1016/j.matpr.2019.05.441

[46]. Veerasamy R, Xin TZ, Gunasagaran S, Xiang TFW, Yang EFC, Jeyakumar N, Arumugam DS. Biosynthesis of silver nanoparticles using mangosteen leaf extract and evaluation of their antimicrobial activities. J Saudi Chem Soc. King Saud University; 2011;15: 113–120. doi:10.1016/j.jscs.2010.06.004

[47]. Wing, Ivanova EP, Nguyen SH, Webb HK, Hasan J, Truong VK. Molecular organization of the nanoscale surface structures of the dragonfly *Hemianax papuensis* wing epicuticle. PLoS One. 2013;8. doi:10.1371/journal.pone.0067893

[48]. Yugandhar P, Haribabu R, Savithramma N. Synthesis, characterization and antimicrobial properties of green-synthesised silver nanoparticles from stem bark extract of *Syzygium alternifolium* (Wt.) Walp. 3 Biotech. Springer Berlin Heidelberg; 2015;5: 1031–1039. doi:10.1007/s13205-015-0307-4

[49]. Zhang QX, Zhang Y, Shan HH, Tong YH, Chen XJ, Liu FQ. Isolation and identification of antifungal peptides from *Bacillus amyloliquefaciens* W10. Environ Sci Pollut Res; 2017;24: 25000–25009. doi:10.1007/s11356-017-0179-8

549 **Figure 1 (a)** *Mang Mao* insect. (**b)** (1) Silver nitrate solution; (2) *Mang Mao* wings extract;
550 (3) Silver nanoparticles; (**c)** UV-Vis spectra of AgNPs synthesized by *Mang Mao* wings
551 extract.

552 **Figure 2 (a)** UV–vis spectra of aqueous silver nitrate concentration. (**b)** Concentration ratio
553 of *Mang Mao* extract with 1 mM silver nitrate. (**c)** Different pH range. (**d)** Different time
554 intervals

555 **Figure 3** SEM images (**a)** pH-3. (**b)** pH-5. (**c)** pH-7. (**d)** pH-9. (**e)** pH-11

556 **Figure 4 (a)** Energy dispersive X-ray analysis of the synthesized MMAgNPs. (**b)** XRD
557 pattern of biosynthesized silver nanoparticles using *Mang Mao* wings extract.

558 **Figure 5** Characterization of MMAgNPs by (a) DLS size distribution and (b) zeta potential
559 analysis

560 **Figure 6** FTIR pattern of the *Mang Mao* wings extract and synthesized MMAgNPs

561 **Figure 7 (a)** TLC of *Mang Mao* wings extract: (1) UV visualization, (2) Ninhydrin reagent.
562 (**b)** SDS-PAGE analysis of *Mang Mao* wings extract protein; Lane 1. Molecular size marker;
563 lane 2. Crude protein; lane 3. Purified protein (46 kDa) responsible for active biosynthesized
564 MMAgNPs

565 **Figure 8** Antioxidant activity: (**a)** DPPH scavenging activity. (**b)** Ferric reducing antioxidant
566 activity.

567 **Figure 9** Antimicrobial activity of synthesized MMAgNPs

568

569

570

Fig.1

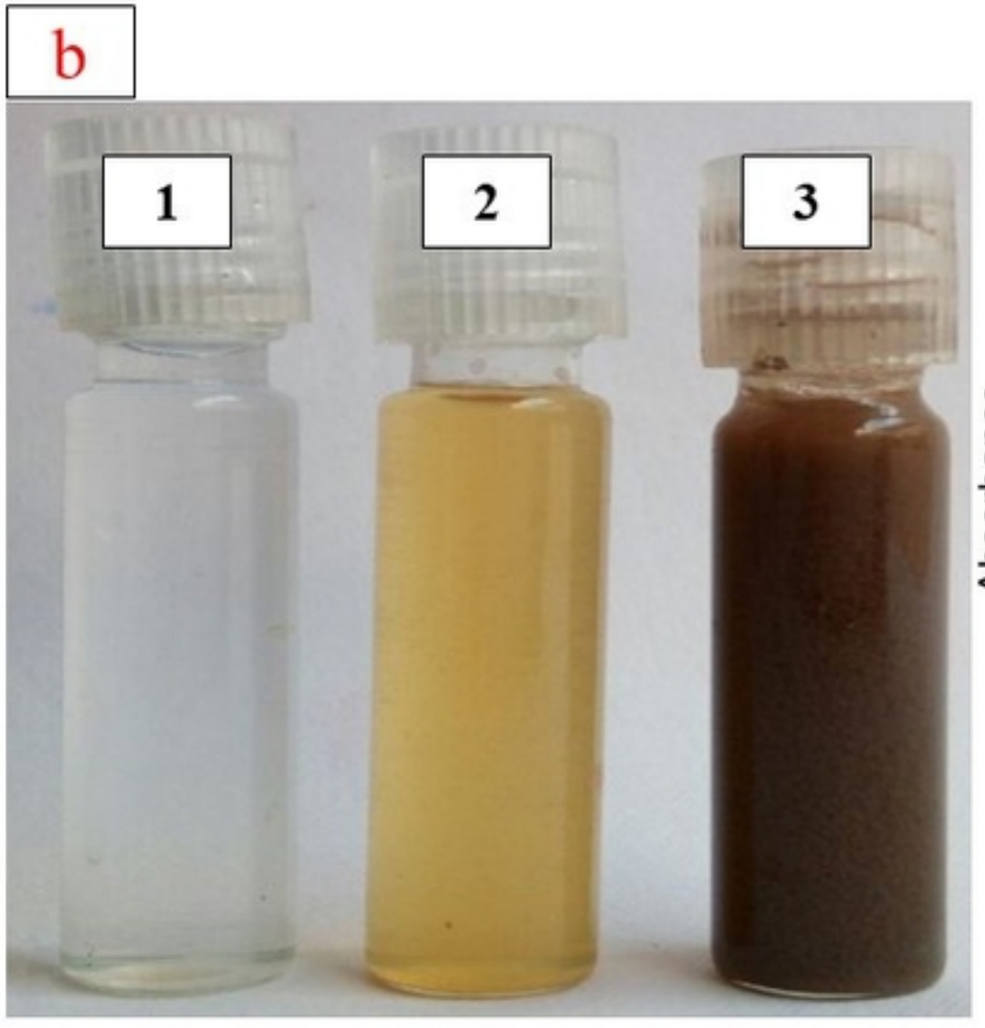

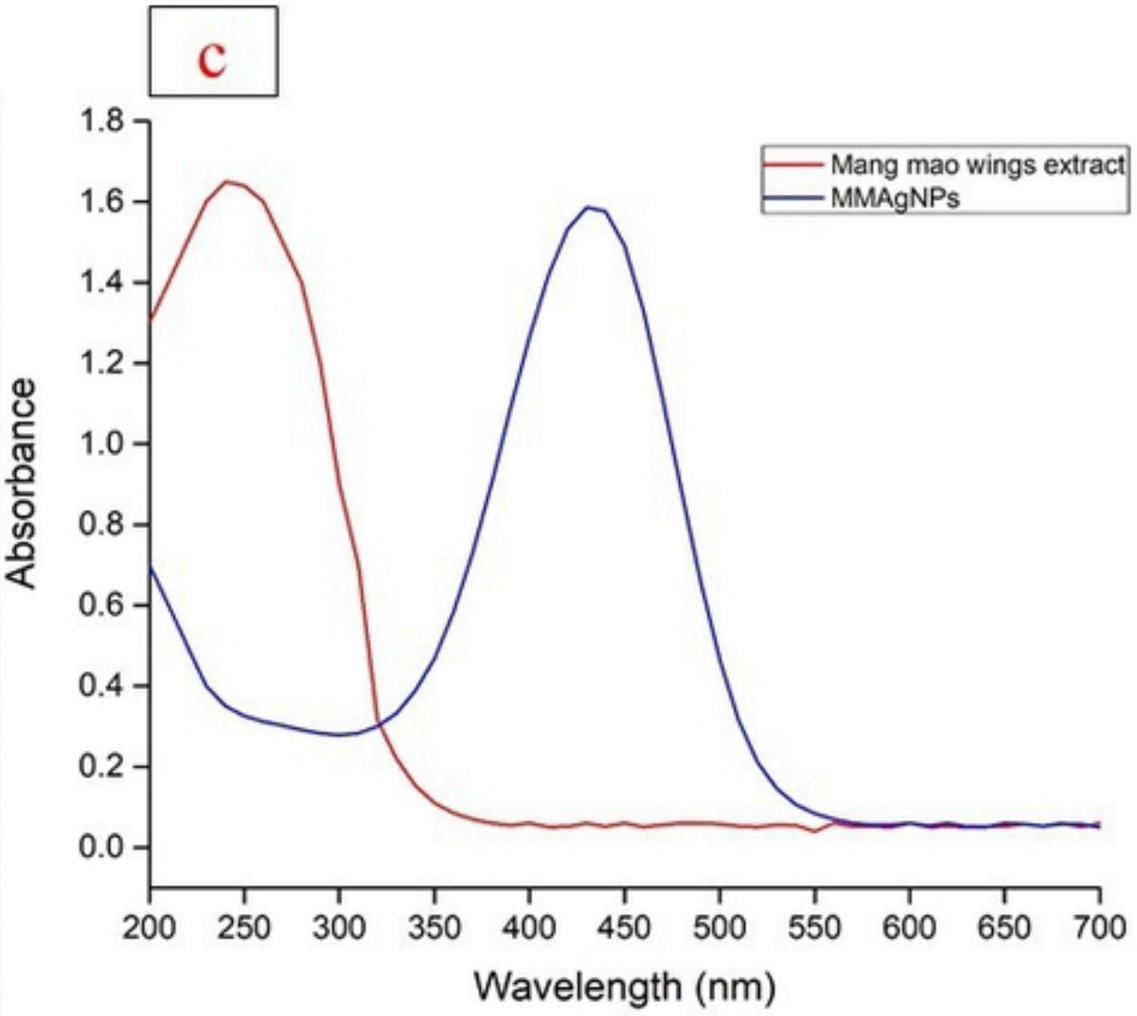

Figure 1

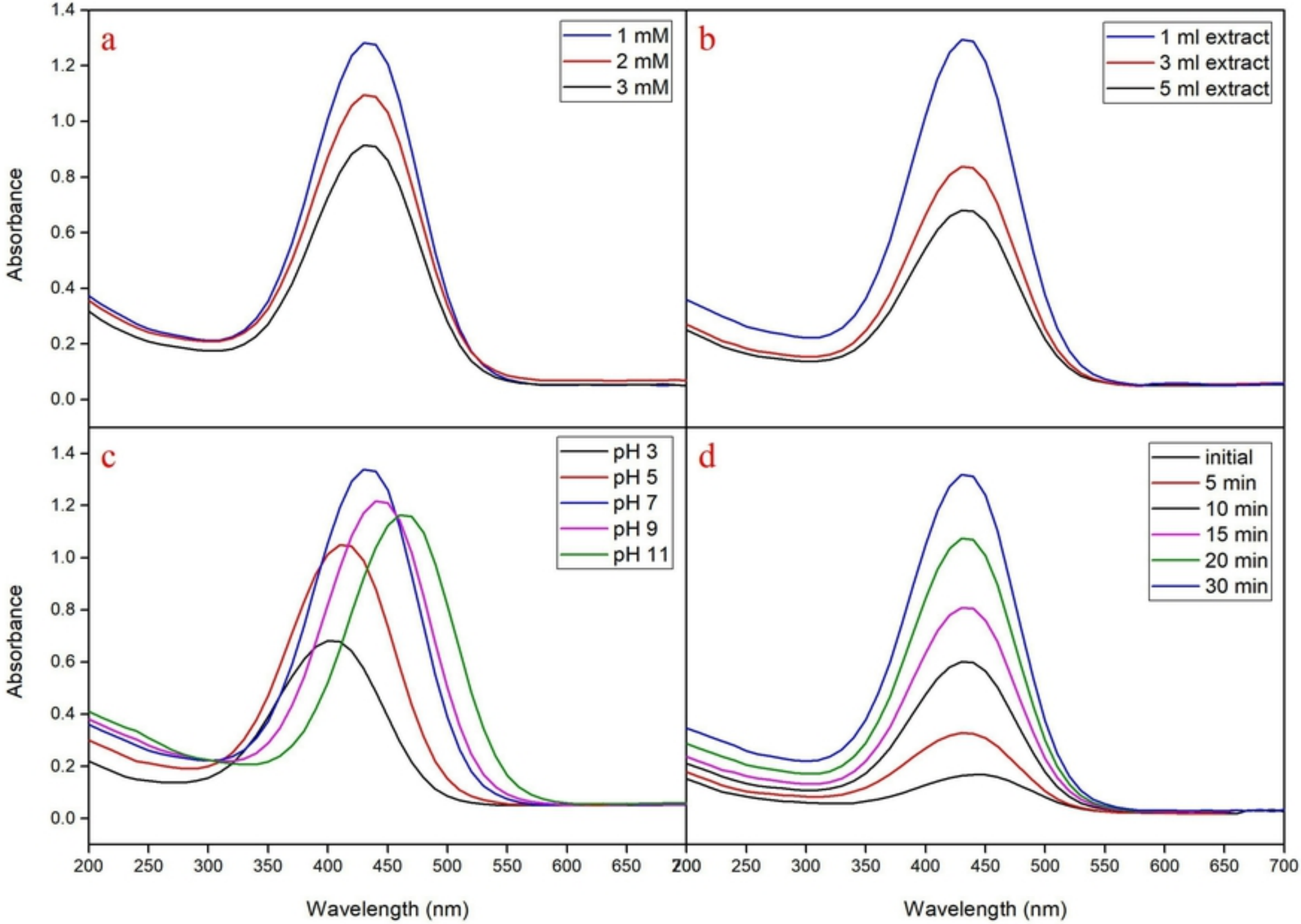
a
1 mM
2 mM
3 mM
b
1 ml extract
3 ml extract
5 ml extract
c
pH 3
pH 5
pH 7
pH 9
pH 11
d
initial
5 min
10 min
15 min
20 min
30 min
Absorbance
Wavelength (nm)

Figure 2

Fig 3.

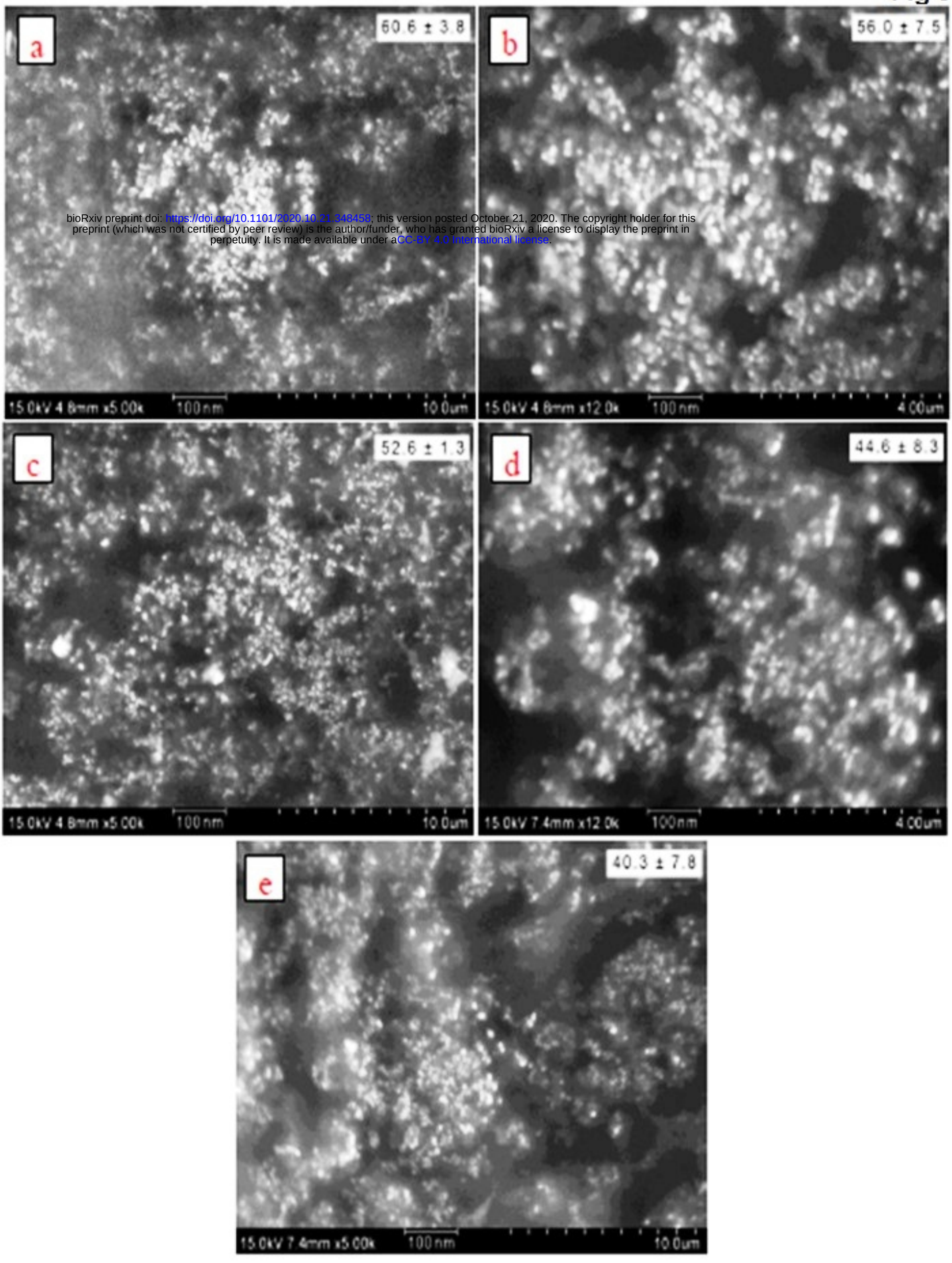

Figure 3

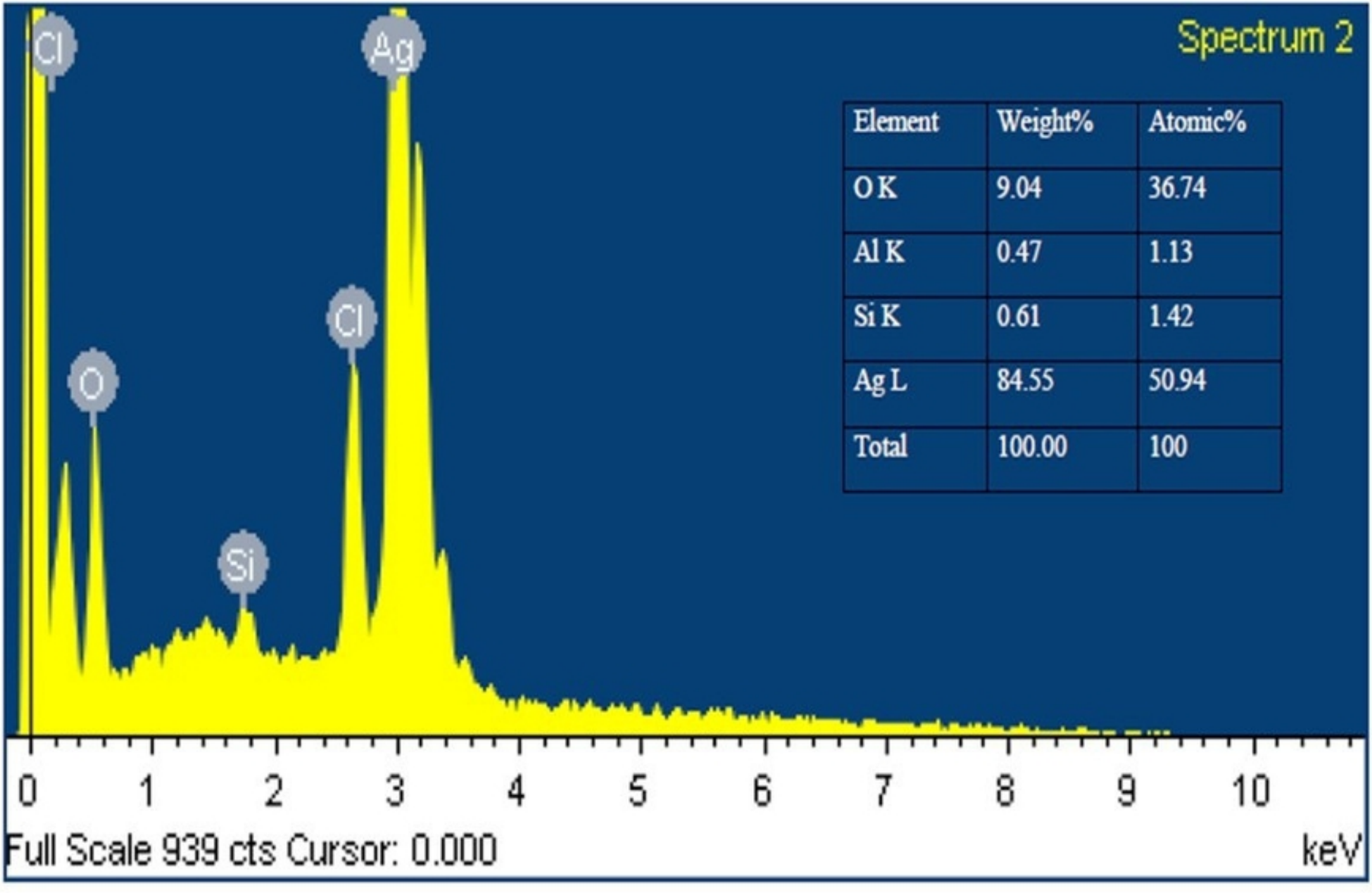
Spectrum 2
Cl
Ag
Cl
O
Si
Element | Weight% | Atomic%
O K | 9.04 | 36.74
Al K | 0.47 | 1.13
Si K | 0.61 | 1.42
Ag L | 84.55 | 50.94
Total | 100.00 | 100
0 1 2 3 4 5 6 7 8 9 10
Full Scale 939 cts Cursor: 0.000
keV

Figure 4a

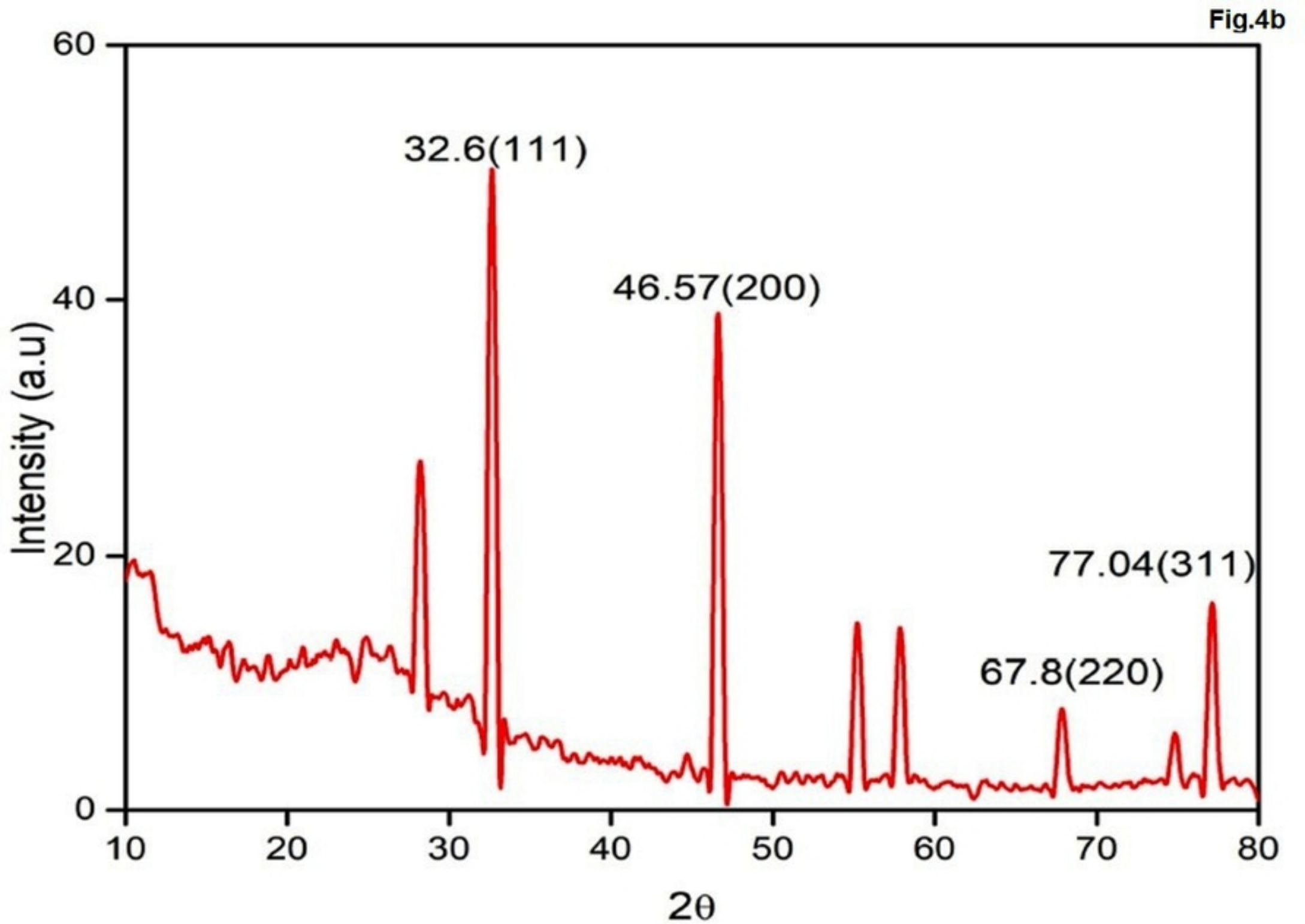
Fig.4b
60
40
20
0
Intensity (a.u)
32.6(111)
46.57(200)
77.04(311)
67.8(220)
10
20
30
40
50
60
70
80
2θ

Figure 4b

Fig.5a

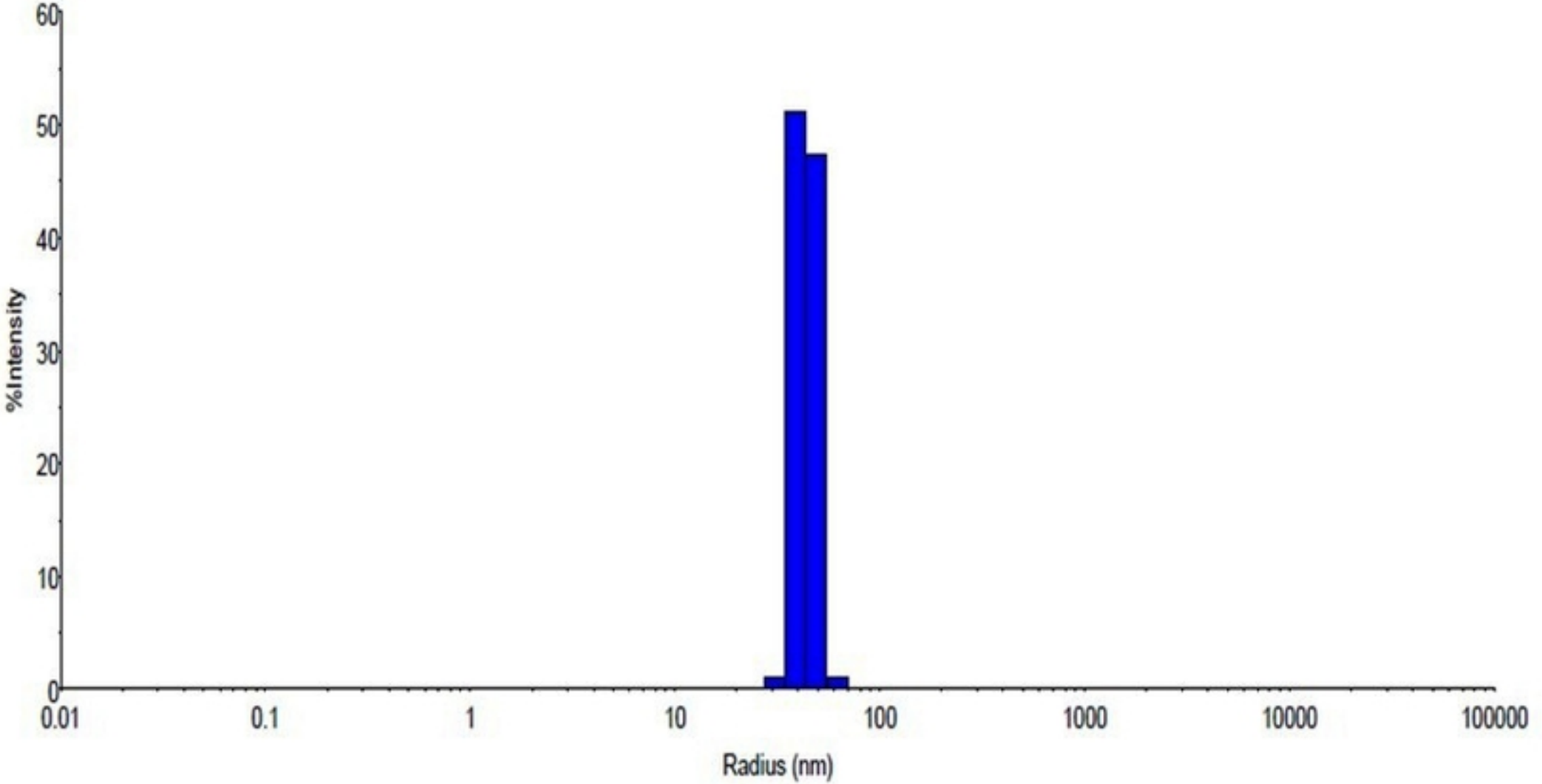

	Radius	Mw-R	%Pd	%Intensity	%Mass	%Number
	(nm)	(kDa)				
Peak 1	43.9	23461.4	12.8	100.0	100.0	100.0

Figure 5a

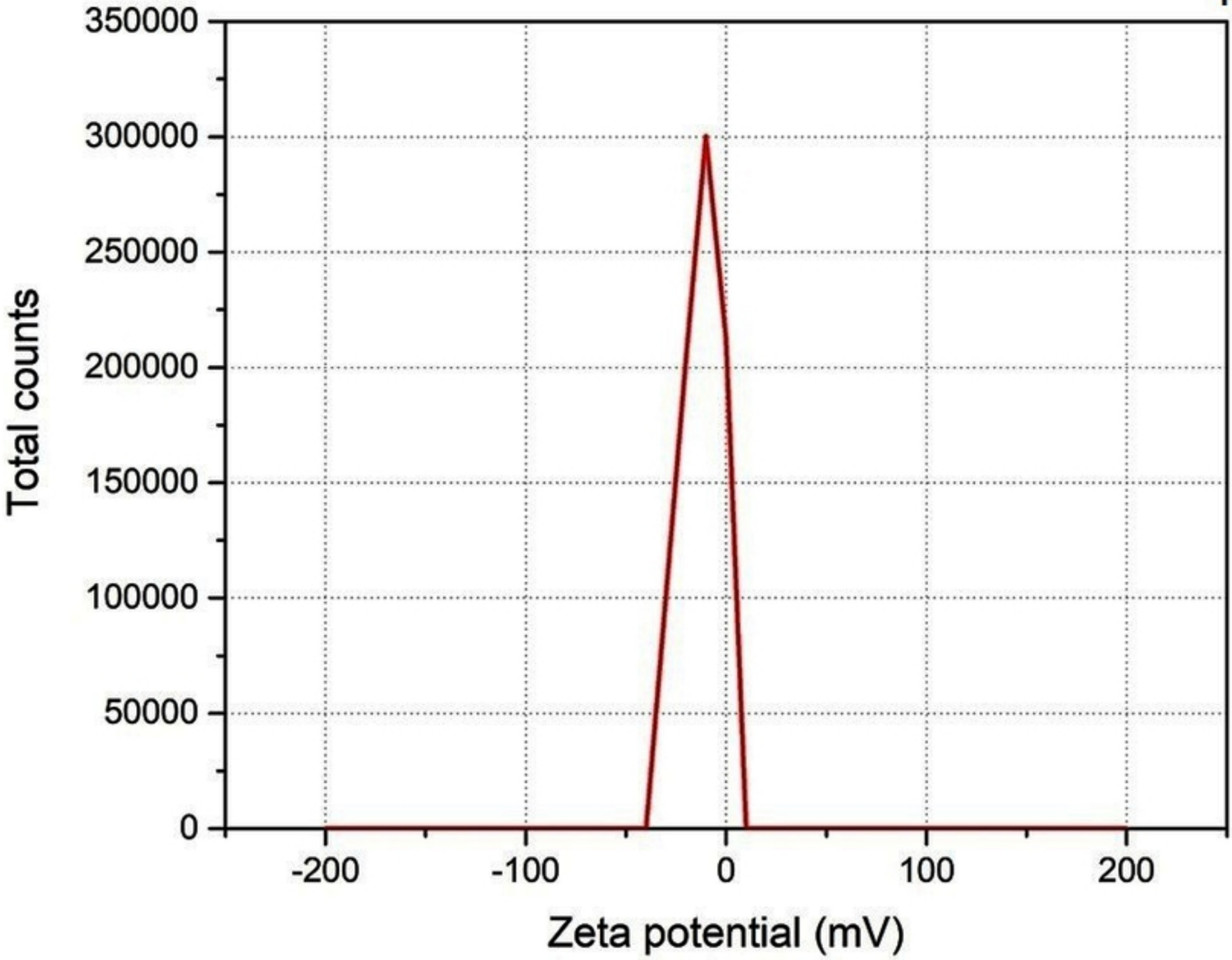
350000
300000
250000
200000
150000
100000
50000
0
Total counts
-200
-100
0
100
200
Zeta potential (mV)

Figure 5b

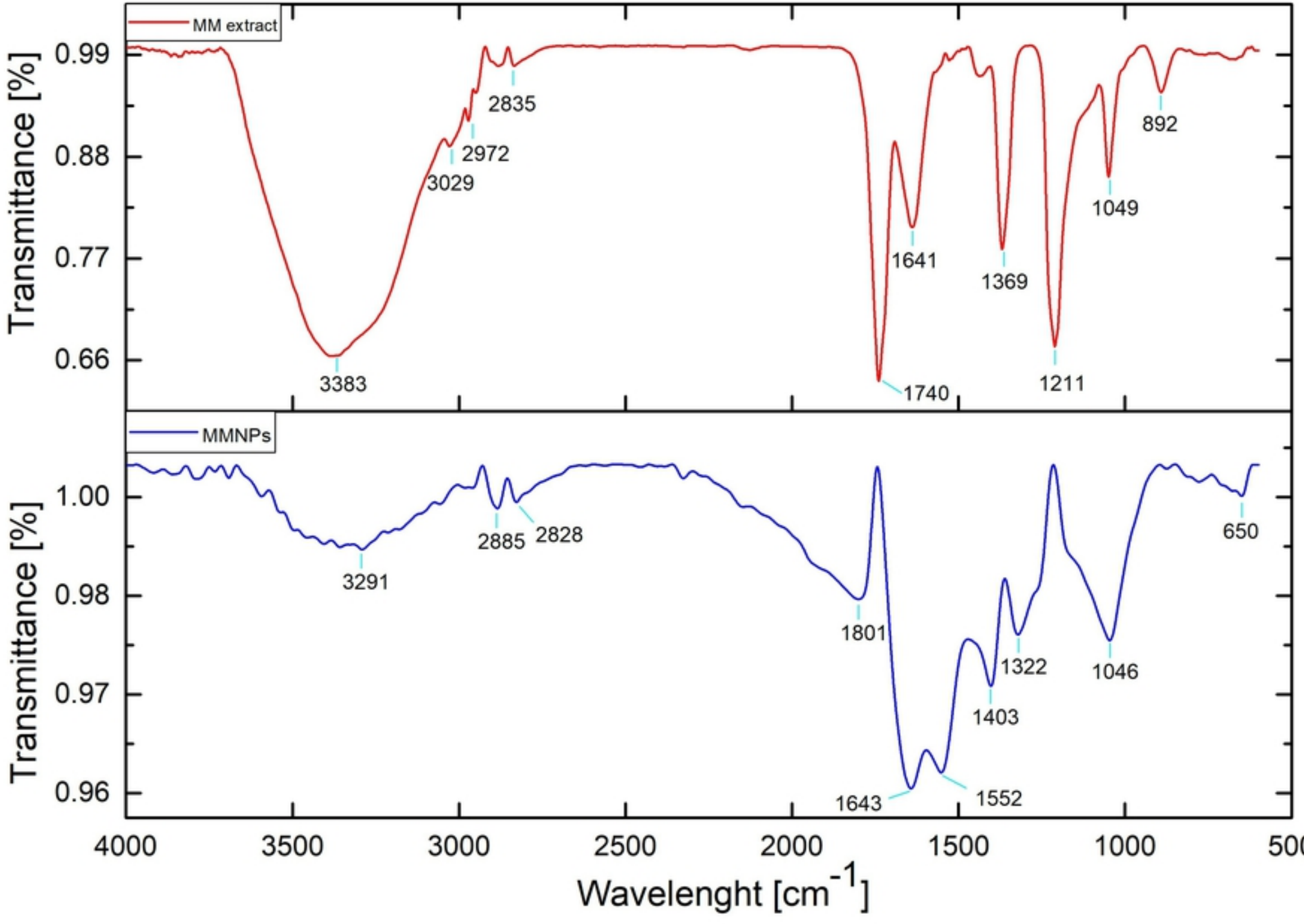
MM extract
Transmittance [%]
0.99
0.88
0.77
0.66
3383
3029
2972
2835
1740
1641
1369
1211
1049
892
MMNPs
Transmittance [%]
1.00
0.98
0.97
0.96
3291
2885
2828
1801
1643
1552
1403
1322
1046
650
4000
3500
3000
2500
2000
1500
1000
500
Wavelenght [cm-1]

Figure 6

Fig. 7.

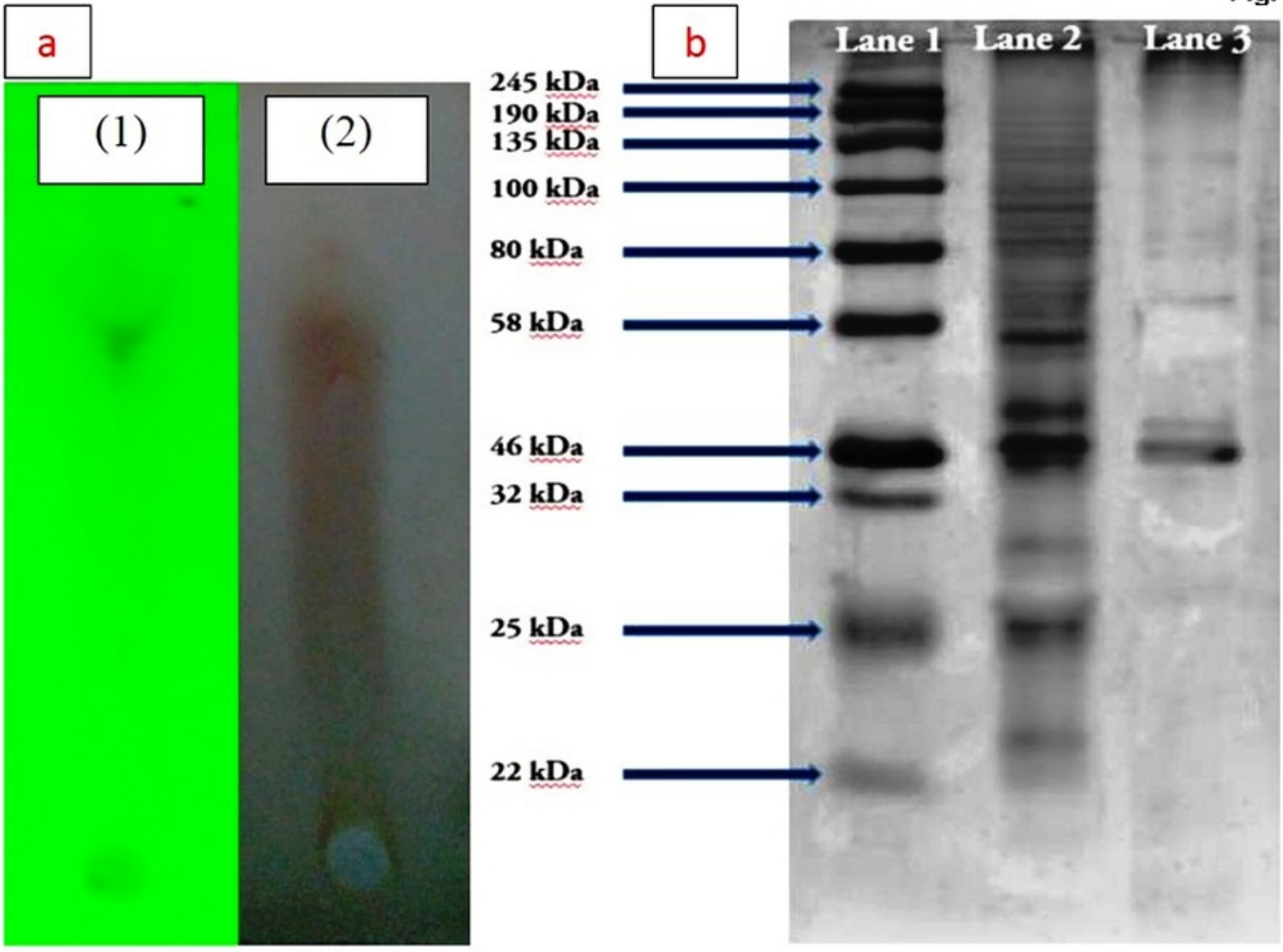

Figure 7

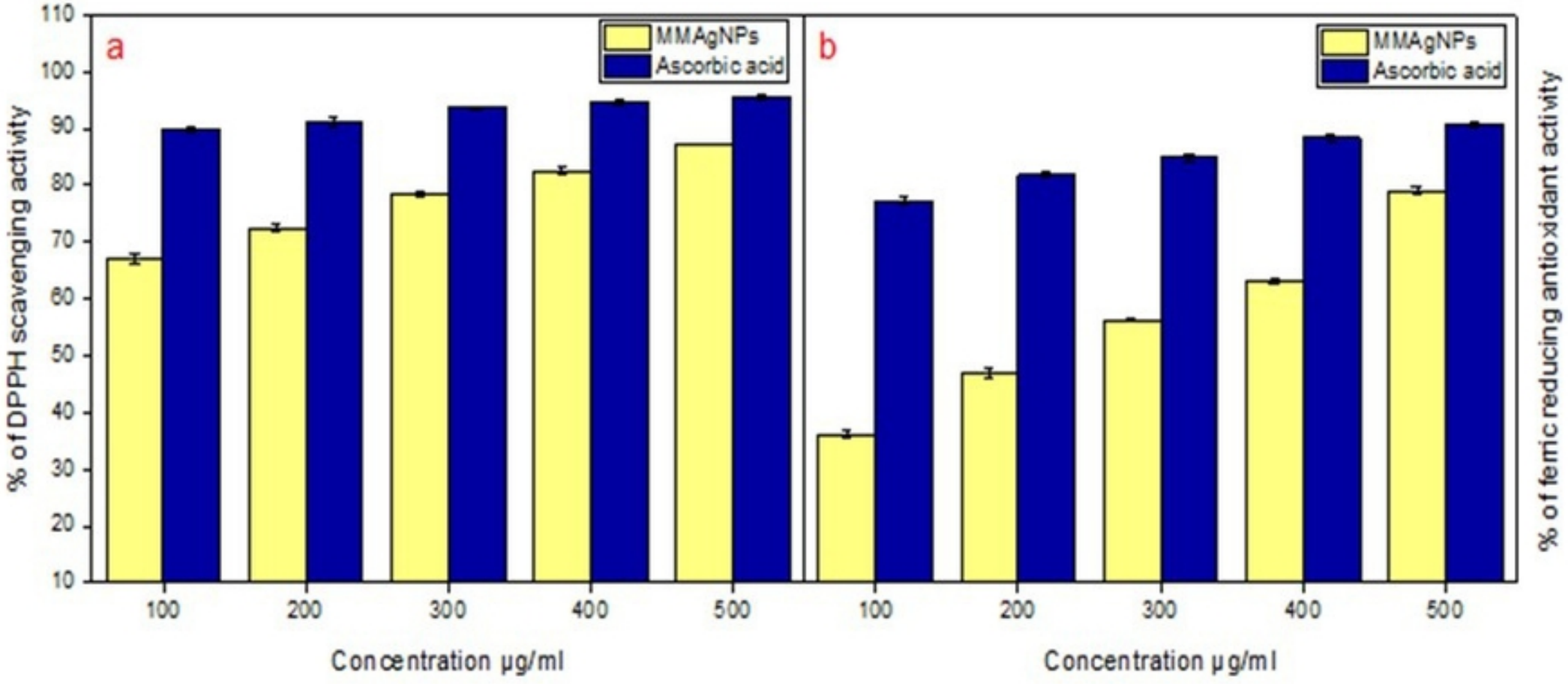
a
b
MMAgNPs
Ascorbic acid
% of DPPH scavenging activity
% of ferric reducing antioxidant activity
Concentration µg/ml
Concentration µg/ml
110
100
90
80
70
60
50
40
30
20
10
100
200
300
400
500

Figure 8

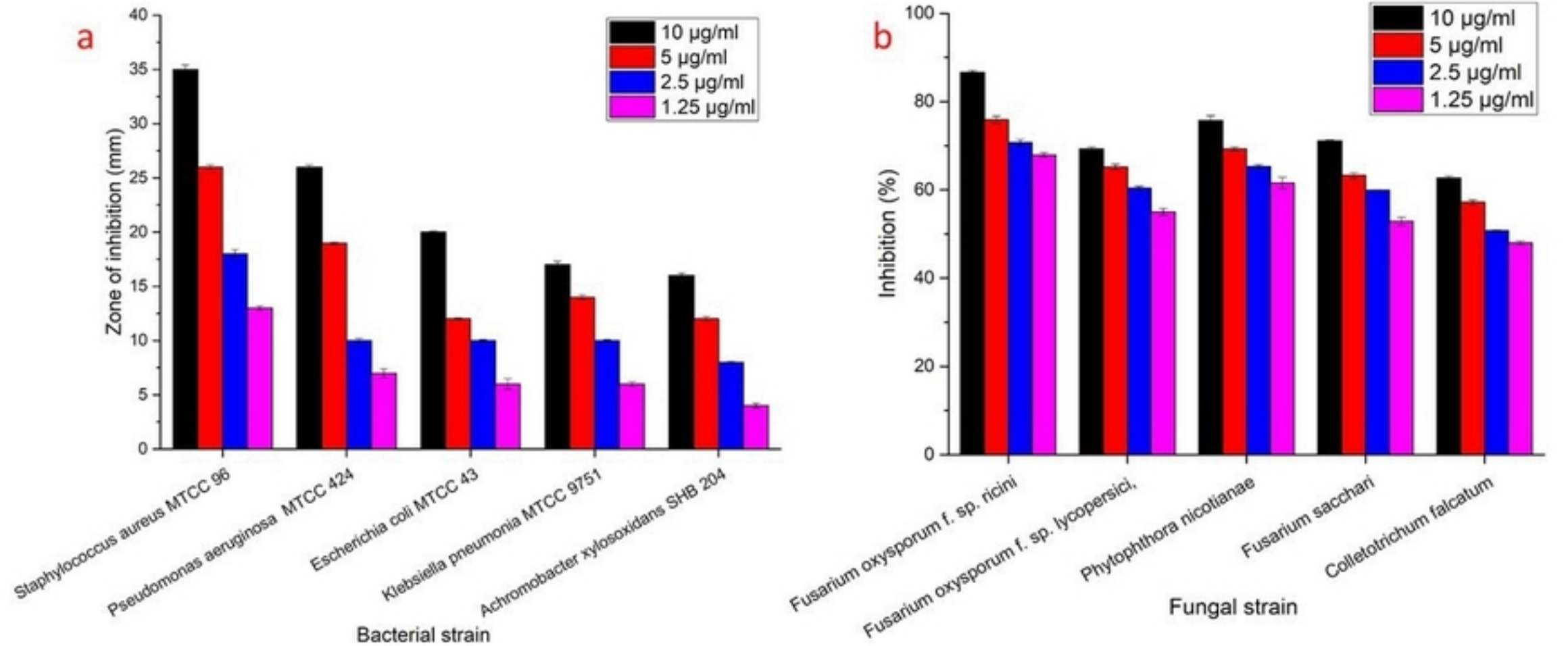
a
Zone of inhibition (mm)
0
5
10
15
20
25
30
35
40
10 µg/ml
5 µg/ml
2.5 µg/ml
1.25 µg/ml
Staphylococcus aureus MTCC 96
Pseudomonas aeruginosa MTCC 424
Escherichia coli MTCC 43
Klebsiella pneumonia MTCC 9751
Achromobacter xylosoxidans SHB 204
Bacterial strain
b
Inhibition (%)
0
20
40
60
80
100
10 µg/ml
5 µg/ml
2.5 µg/ml
1.25 µg/ml
Fusarium oxysporum f. sp. ricini
Fusarium oxysporum f. sp. lycopersici,
Phytophthora nicotianae
Fusarium sacchari
Colletotrichum falcatum
Fungal strain

Figure 9